A Connection Between Star Formation Rate and Dark Matter Halos at $Z \sim 6$ In 2013 Planck Cosmology.

F.L. Gómez-Cortés[1]

Departamento de Fsica, Universidad de los Andes, Colombia

Received _____; accepted _____

ABSTRACT

This work relates baryonic matter and dark matter at redshift $z = 5.9$ using observational data from CFHTLS (Willott 2013), HUDF09 (Bouwens 2006, 2012), UKIDSS and SDXS (McLure 2009), and results of the Multidark Simulation (Riebe 2013) in a cubic box of 1000Mpc h^{-1} length with 2013 Planck Cosmology. The Luminosity Function (LF) is fitted via four parameters with the Markov Chain Monte Carlo method. The relationship between the Dark Matter Halos Mass and Star Formation Rate is obtained using the relationship between the UV continuum (from the fitted LF) and Star Formation Rate (SFR) by Kennicutt (1998).Cosmic variance effects are studied on smaller boxes of 250Mpc h^{-1} length.

Halos.

Subject headings: Dark Matter, LF, SFR, High Redshift Galaxies, Reionization

1. Introduction

Dark matter is a significative component of the universe.

(Trimble 1987)

Hierarchy Structure Evolution: Early formation of small structures merging on major structures after.

From simulations, Halo Mass Function as function of redshift (or time).

Star formation rate as function of time. Peak at $z \sim 2$.

Main Objetive: Reproduce the observed luminosity function at redshift $z = 5.9$ from a DMH catalog from simulations.

1.1. Halo Mass Function (HMF)

The HMF is created using the DMH catalog from the Multidark Database (Riebe 2013).

1.2. Cosmic Variance

Is important to know and understand the existence of local fluctuations or inhomogeneities due the observed scale. For this part is necesary to study the HMF on smaller boxes

2. Relationship between Galaxy Luminosity Function (GLF) and Dark Matter Halo (DMH) mass

In one hand we have observational results: the GLF for star-forming galaxies at high redshift (z=5.9)(Bouwens 2006; Willott 2013) expressed in terms of magnitude in the ultraviolet range (M1350). In the other hand we have a DMH catalog, result from the Multidark Simulation with Plank Cosmology.

A 1000 $\mathrm{Mpc^3h^3}$ cubic box containing near to 11×10^6 dark matter halos.

The idea is to connect the observed GLF with the DMH catalog. We assume that each halo contains one and just one galaxy, and its luminosity is given by:

$$L_{\mathrm{galaxy}} = \alpha M_{\mathrm{halo}}^{\beta} \tag{1}$$

but this function is given in magnitude units. Is necesary to convert magnitude to luminosity.

2.1. Magnitude to Luminosity

The Luminosity is an intrinsic propertie of the stars. It doesn't deppends of the distance. It's directly related to the energy flux emmited. The luminosity L_ν at a given frecuency ν has $[\mathrm{WHz^{-1}}]$ or $[\mathrm{ergs^{-1}Hz^{-1}}]$ units.

The magnitude is brightnes star classification inherited from ancient Greeks. It deppends of the stellar distance. The absolute magnitude is a modern classification independent of distance. Taking the Sun as reference, the absolute magnitud at a given wavelengt is given by:

$$M_\lambda = M_{\lambda\odot} - 2.5 \log_{10}\left(\frac{L_\lambda}{L_{\lambda\odot}}\right)$$

The solar absolute magnitude in the U filter is $M_{U\odot} = 5.61$, and the solar luminosity in the same filter is $L_{U\odot} = 10^{18.48}$ergs s^{-1}Hz^{-1} or $L_{U\odot} = 3.02 \times 10^{18}$ergs s^{-1}Hz^{-1}.

Replacing in the absolute magnitude equation:

$$M_U = 5.61 - 2.5 \log_{10}(L_U) + 2.5 \times 18.48$$

gives the magnitude in the U filter of an astrophysical source:

$$M_U = 51.82 - 2.5 \log_{10}(L_U)$$

2.2. Best Fitting Parameters

3. Star Formation Rate

On the study of far galaxies individual stellar spectrum is unresolved, is not possible to make a detailed census of the galaxy popullation. Only is possible to get information from the whole stellar population, an integrated spectrum.

Kennicutt pruposed a method in wich a linear relation between luminosity and SFR can be assumed. This model allows to estimate the young stars fraction and the mean SFR over periods of $10^8 - 10^9$yr. The luminosity in the modfel, comes from the UV and the FIR broadband, also from speciffic recombination lines.

In a typical galaxy spectrum the visible wavelengths are dominated by the main sequence stars (A to early F) and G-K giants. In few wavelength ranges we have a significative contribution from the young stars rather than the old stars. The infrared and far infrared wavelengths emission is dominated by dust, this dust is heated by the whole stellar popullation, in particular by young, UV-bright stars (Law 2011).The UV broadband emission is dominated by blue stars with temperature near to 40.000K. These hot and massive stars has a lifetime of 10^8Gyr, they spend their nuclear fuel faster than smaller and cooler sunlike stars.

The relation between UV luminosity and Star Formation Rate (Kennicutt 1998) is given by: $\mathrm{SFR}\,(M_\odot \mathrm{yr}^{-1}) = 1.4 \times 10^{28} L_\nu \left(\mathrm{erg\ s^{-1}Hz^{-1}}\right)$ With Initial Mass Function (IMF) between $0.1M_\odot$ and $100M_\odot$, in the range of $1250 - 2500$Å

The UV dust absorption (Kennicutt 2009) is not taken account in this work.

4. The Fitting Model

This fitting model contains four parameters: $(m/M)_0$, M_1, β and γ, where $m :=$ Stellar mass, and $M :=$ Dark Matter Halo mass.

$$\frac{m}{M} = 2\left(\frac{m}{M}\right)_0 \left[\left(\frac{M}{M_1}\right)^{-\beta} + \left(\frac{M}{M_1}\right)^{\gamma}\right]^{-1} \tag{2}$$

This is similar to the proposed by Moster (2010). Another model cited in the article contains five parameters: m_0, M_1, β, γ_1 and γ_2.

$$m(M) = m_0 \frac{(M/M_1)^{\gamma_1}}{[1 + (M/M_1)^{\beta}]^{(\gamma_1 - \gamma_2)/\beta}}$$

"We use a statistical approach to determine the relationship between the stellar masses of galaxies and the masses of the dark matter halos in which they reside. We obtain a parameterized stellar-to-halo mass (SHM) relation by populating halos and subhalos in an N-body simulation with galaxies and requiring that the observed stellar mass function be reproduced." (Moster 2010)

5. Observations

The dataset was retrieved from graphs for Bouwens (2014) and McLure (2009) using DEXTER http://dc.zah.uni-heidelberg.de/dexter/ui/ui/custom

5.1. CFHTLS

CFHTLS - Canada-France-Hawaii Telescope Legacy Survey - MegaCam(Willott 2013)

"We identify a sample of 40 Lyman break galaxies brighter than magnitude z = 25.3 across an area of almost 4 square degrees. Sensitive spectroscopic observations of seven galaxies provide redshifts for four, of which only two have moderate to strong Ly emission lines. All four have clear continuum breaks in their spectra." Willott (2013).

"The imaging data used to select high-redshift galax- ies come primarily from the 3.6 m Canada-France-Hawaii Telescope. Optical observations with MegaCam in the u g r i z filters are from CFHTLS Deep which covered four 1 square degree fields with typical total integra- tion time of 75 ks in u , 85 ks in g , 145 ks in r , 230 ks in i and 175 ks in z . The seeing in the final stacks at i and z range from 0.66 to 0.76 arcsec. The data used here are from the 6th data release, T0006, which contains all the data acquired over the five years of the project " Willott (2013).

"These optical data are complemented by near-IR data from the WIRCam Deep Survey (WIRDS; Bielby et al. 2012). WIRDS used the WIRCam near-IR imager at the CFHT" Willott (2013).

About the Luminosity function: sect 6.3 "Because our LBG sample covers only a limited range of apparent and absolute magnitudes, we cannot use it to determine the full galaxy luminosity function at z = 6. The luminosity function at the break and at fainter

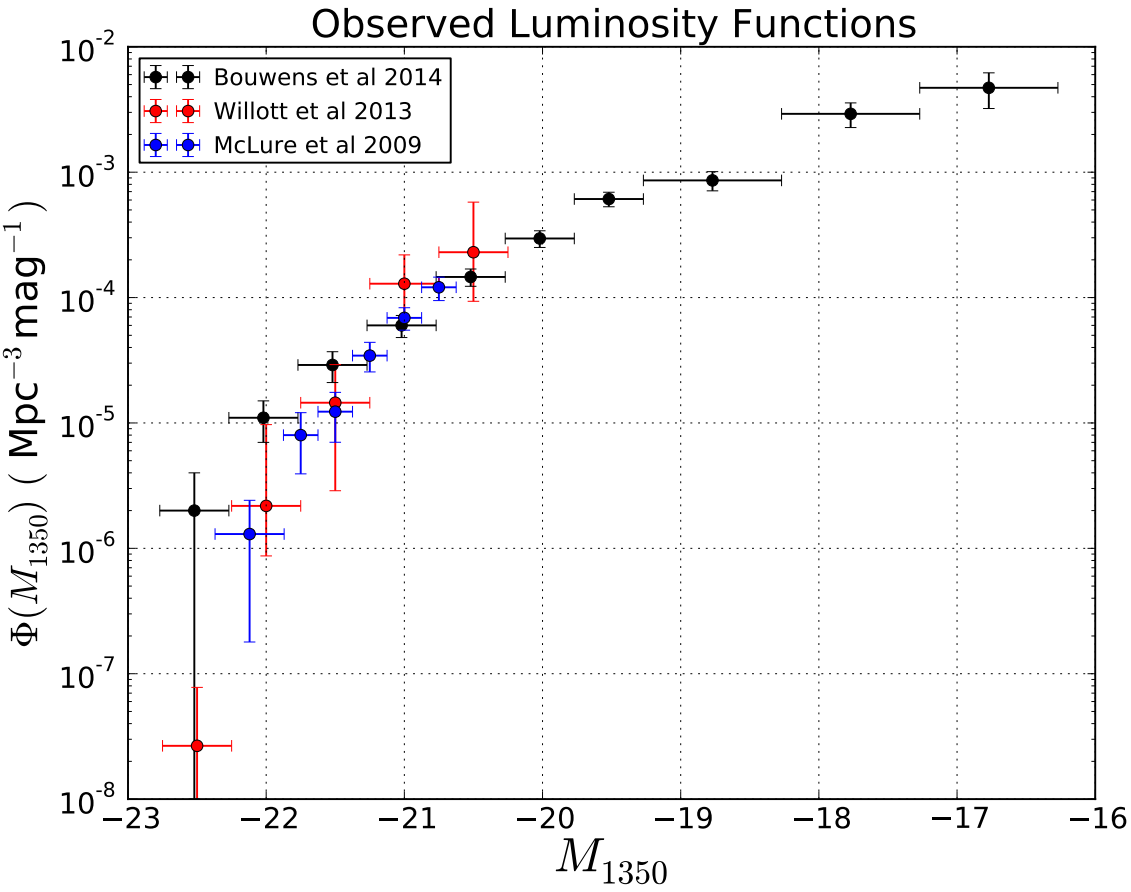

Fig. 1.— Observational data from Bouwens (2014); McLure (2009)and Willott (2013).

magnitudes has already been well studied from deep HST surveys over small sky areas (Bouwens et al. 2007). The main contribution of our study is to determine the space density of very rare, highly luminous LBGs."Willott (2013).

5.2. HUDF09

"Table 1 summarizes the search fields used for the z 5- 8 LF determinations and the approximate depths of the available ACS+WFC3/IR observations. Our primary data set consists of the full two-year WFC3/IR obser- vations of the HUDF and two flanking fields obtained with the 192-orbit HUDF09 program (PI Illingworth: GO 11563). Our second data set is the 145 arcmin 2 ACS+WFC3/IR observations over the wide-area Early Release Science (Windhorst et al. 2011) and CDF-South CANDELS" Bouwens (2012)

"A detailed summary of the ACS HUDF, HUDF-Ps, and GOODS data we use for our dropout selections is provided in our previous work (B06). Nevertheless, a brief description of the data is in- cluded here. The ACS HUDF data we use are the version 1.0 re- ductions of Beckwith et al. (2006) and extend to 5 point-source limits of 29Y30 in the B 435 V 606 i 775 z 850 bands. The HUDF-Ps re- ductions we use are from B06 and take advantage of the deep (k72 orbit) BViz ACS data fields taken in parallel with the HUDF NICMOS program (Thompson et al. 2005). Together the parallel data from this program sum to create two very deep ACS fields that we can use for dropout searches. While of somewhat var- iable depths, the central portions of these fields (12Y20 arcmin 2) reach some 0.6Y0.9 mag deeper than the data in the original ACS GOODS program (Giavalisco et al. 2004a). Finally, for the ACS GOODS reductions, we use an updated version of those generated for our previous z 6 study (B06)." Bouwens (2006)

5.3. UKIDSS & SDXS

"The UDS is the deepest of five near-IR surveys currently underway at the UK InfraRed Telescope (UKIRT) with the new WFCAM imager (Casali et al. 2007) which together comprise the UKIDSS (Lawrence et al. 2007). The UDS covers an area of 0.8 deg 2 cen- tred on RA = 02:17:48, Dec. = 05:05:57 (J2000) and is already the deepest, large area, near-IR survey ever undertaken. The data utilized in this paper were taken from the first UKIDSS Data Re- lease (DR1; Warren et al. 2007), which included JK imaging of the entire UDS field to 5 depths of J = 23.9, K = 23.8 (1.6 arcsec diameter apertures). The UKIDSS DR1 became publicly available to the world wide astronomical community in 2008 January and can be downloaded from the WFCAM Science Archive. 2 The UDS field is covered by a wide variety of deep, multiwave- length observations ranging from the X-ray through to the radio (see Cirasuolo et al. 2008 for a recent summary). However, for this study the most important multiwavelength observations are the deep op- tical imaging of the field taken with Suprime-Cam (Miyazaki et al. 2002) on Subaru as part of the Subaru/XMMNewton Deep Survey (Sekiguchi et al. 2005). The optical imaging consists of five over- lapping Suprime-Cam pointings, and covers an area of 1.3 deg 2 . The whole field has been imaged in the BV Ri z filters, to typical 5 depths of B = 27.9, V = 27.4, R = 27.2, i = 27.2 and z = 26.2 (1.6 arcsec diameter apertures). The reduced optical imaging of the SXDS is now publicly available 3 and full details of the observations, data reduction and calibration procedures are provided in Furusawa et al. (2008). The high-redshift galaxies investigated in this study were selected from a contiguous area of 0.63 deg 2 (excluding areas contaminated by bright stars and CCD blooming) covered by both the UDS near-IR and SXDS optical imaging." McLure (2009)

5.4. The Drop-out Technique - Lyman Break Technique

Steidel (2003)

6. Discussion

Q: Mpc/h ?

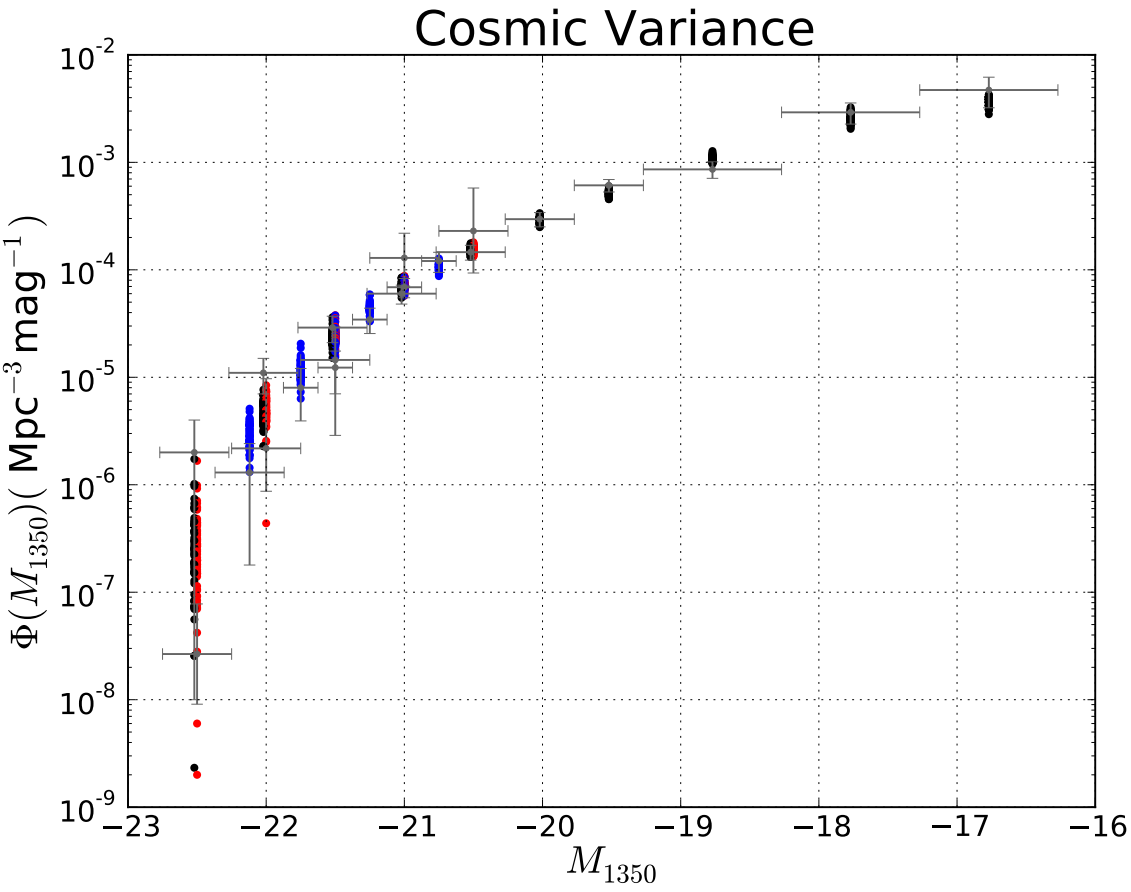

Fig. 2.— Cosmic Variance: The Luminosity Function is made using the DMH catalog from the full box and the set of parameters from the small boxes.

7. Summary

A. Appendix material

DEXTER http://dc.zah.uni-heidelberg.de/dexter/ui/ui/custom

REFERENCES

Bouwens, R. J. et al. 2006, ApJ, 653, 53

Bouwens, R. J. et al. 2012, ApJ, 752, 5

Bouwens, R. J. et al. 2012, arXiv:1403.4295

Kennicutt, Robert C., Jr. 1998, ARA&A, 36, 189

Kennicutt, Robert C., Jr et al. 2009, ApJ, 703, 4672

Law, K. et al. 2011, ApJ, 738, 124

McLure, R. J. et al. 2009, MNRAS, 395, 2196

Moster, Benjamin P. et al. 2010, ApJ, 710, 903

Riebe, K. et al. 2013, AN, 334, 691

Steidel, Charles C. et al. 2003, ApJ, 592, 728

Trible, Virginia. 1987, ARA&A, 25, 425

Willott, Chris J. et al. 2013, AJ, 145, 4